Open access • Journal Article • DOI:10.1063/1.1759393

Structural and magnetic model of self-assembled FePt nanoparticle arrays

Thomas Thomson, Michael F. Toney, Simone Raoux, Stephen Lee ...+3 more authors

Published on: 30 Jun 2004 - Journal of Applied Physics (American Institute of Physics)

Topics: Magnetic nanoparticles, Magnetic anisotropy, Coercivity, Nanoparticle and Magnetic core

SLAC-PUB-10450
May 2004

Structural and magnetic model of self-assembled FePt nanoparticle arrays

T. Thomson
Hitachi San Jose Research Center, 650 Harry Road, San Jose, California 95120, USA

M.F. Toney
Stanford Synchrotron Radiation Laboratory, SLAC, Menlo Park, California 94025, USA

S. Raoux
IBM – Almaden Research Center, 650 Harry Road, San Jose, California 95120, USA

S.L. Lee
School of Physics and Astronomy, University of St. Andrews, St. Andrews, Fife KY16 9SS, UK

S. Sun and C.B. Murray
IBM – T.J.Watson Research Center, Yorktown Heights, New York 10598, USA

B.D. Terris
Hitachi San Jose Research Center, 650 Harry Road, San Jose, California 95120, USA

Abstract

Chemically ordered, self-assembled FePt nanoparticle arrays with high magnetic anisotropy are considered a candidate medium for data storage beyond 1 Tbit/in^2. We report comprehensive structural and magnetic studies on thin (3 layer) assemblies of polyethylenimine (PEI) and 4 nm $Fe_{58}Pt_{42}$ nanoparticles using X-ray diffraction, small angle neutron scattering and magnetometry. We show that prior to annealing FePt nanoparticles in the PEI-FePt assembly consist of a metallic, magnetic core surrounded by a weakly magnetic or non-magnetic shell. High temperature annealing creates the

Work supported in part by the Department of Energy Contract DE-AC03-76SF00515

desired $L1_0$ chemical ordering and results in high coercivity FePt nanoparticles. However, we find that the high temperatures necessary to establish full chemical ordering leads to particle sintering and agglomeration. Understanding the magnetic and physical properties of these assemblies allows future research directions to be clarified for nanoparticle arrays as data storage media.

INTRODUCTION

Magnetic nanoparticles are of broad interest in such diverse areas as data storage,[1] permanent magnets,[2] sensors,[3] medical applications,[4-5] and drug delivery systems.[6] Thus advances in understanding the properties of magnetic nanoparticles in one area of endeavor have a broader applicability. The recent fabrication of arrays of 4 nm diameter FePt nanoparticles with an extremely narrow size distribution,[1] has prompted a significant research effort in this area,[7-14] due to their potential technological application as recording media.[15-18] To realize the full potential of nanoparticle arrays as a recording medium, it is necessary to have a detailed physical understanding of the constituent nanoparticles and the nanoparticle arrays. High temperature annealing is required to form the $L1_0$ high anisotropy phase of FePt which allows the possibility of additional thermally activated chemical and physical processes. During annealing one can envisage three such thermally activated processes that might occur. Firstly, there is the desired phase transformation where initially chemically disordered face-centered cubic (fcc) FePt forms the chemically ordered $L1_0$ phase (where planes of Fe and Pt atoms are stacked alternately along the [001] crystallographic direction) leading to high magnetic anisotropy. Secondly, there is the possibility that particles which initially form a well-ordered array can agglomerate and/or sinter into larger entities and, finally, the chemical oxidation state of the Fe in the nanoparticles can also change. Hence, there is an urgent need to understand how these thermodynamic processes affect magnetic and structural properties. We first seek a detailed understanding of the physical and chemical state of the as-deposited particle arrays. We then present results and analysis that describes the

evolution of the structural and magnetic properties as the arrays are annealed and demonstrate the structural origin of the observed magnetic properties. This model of nanoparticle arrays allows us to identify the research challenges that must be met before the technological potential of these arrays can be realized.

II. EXPERIMENTAL

The polymer mediated method described by Sun et al.,[19-20] was used to deposit 3 layers of PEI-FePt nanoparticle arrays onto Si substrates. The precursors of the nanoparticle synthesis were added in a ratio that produces $Fe_{58}Pt_{42}$ nanoparticles which have previously been shown to exhibit the highest coercivity (H_c) after annealing.[1] This technique provides thin arrays consisting of particles with a diameter of ~4nm and an extremely narrow size distribution (< 5%). The PEI-FePt nanocomposite process was used in order produce thin, smooth assemblies over extended areas. Annealing of the thin film arrays was undertaken in N_2 at atmospheric pressure. The annealing conditions employed were 30mins at 580°C, 5mins at 650°C, 5mins at 700°C and 5mins at 800°C.

Small Angle Neutron Scattering (SANS) measurements were undertaken on instrument D11,[21] at the Institut Laue Langevin high flux reactor in Grenoble, France using a neutron wavelength of λ = 4.5Å. The data were collected at three detector positions in order to scan a scattering vector, q, range of 0.0012 – 0.03nm^{-1}. Particle diameters were determined from the q dependence of the scattered intensity by matching the data to simulations of interacting, polydisperse hard spheres in the Percus-Yevick approximation

using the method of Griffith et al.[22] A full description of this work is currently in preparation[23] while a summary maybe found in Ref.[24].

The X-ray diffraction (XRD) measurements were performed in a grazing incidence geometry at the National Synchrotron Light Source using beamline X20C. The diffracted beam was analyzed with 1 milliradian Sollar slits, which provided a finer resolution than any of the diffraction peak widths. The peak widths were analysed to determine particle diameters. The data were also analysed to determine the Warren long-range order parameter S, which is unity for complete chemical order, zero for chemical disorder, and proportional to extent of chemical order for partial order[25] as reported in Ref.[26].

The magnetization data were obtained from hysteresis loops measured on an Oxford Instruments vibrating sample magnetometer (VSM) with a maximum applied field of 9 Tesla. Data were collected over a temperature range of 1.9 to 350K. Non-linear background signals were carefully measured and subtracted for each measurement condition while linear background contributions were determined from fits to the data at high applied fields. The noise floor of the instrument was 2μemu.

III. RESULTS AND DISCUSSION

Figure 1 shows magnetization as a function of applied field at a temperature of T =100K for an unannealed particle array together with an insert that shows magnetization (at 9 Tesla) vs measurement temperature. The solid line is a fit to the Langevin function which describes the response of a 3D random array of uniaxial particles to an applied field. Using a value of M_s = 1030 emu/cm^3 as determined from *ab initio* calculations

and experiment,[27-28] (and refs therein) for a chemically disordered fcc $Fe_{0.5}Pt_{0.5}$ alloy, a particle diameter of 2.2 nm is required to match the observed temperature dependence of magnetization at all temperatures above 20K. This diameter is significantly smaller than the 4.5 nm measured by SANS but is in good agreement with the diameter of 2.2nm determined by XRD, as shown in Fig. 2. These data are easily explained by considering the differences between SANS and XRD. XRD data are analyzed by determining the width of the peaks from well defined crystallographic planes, in this case the (111) planes. SANS merely requires a contrast in neutron scattering length density and hence would be less sensitive to thin surface layers such as an oxide. The data suggests a model whereby a large fraction of the as-deposited particles consist of a metallic core of chemically disordered fcc FePt with a fairly narrow distribution of sizes centered at a diameter of 2.2nm surrounded by a non- or weakly magnetic Fe-containing oxide layer. This model is strongly supported by NEXAFS data taken on the same samples at the Fe L edge and described by Anders et al.[26] The NEXAFS data for the unannealed array show little or no contribution from Fe in a metallic environment which, due of the surface sensitivity of the technique, can be modeled in terms of an oxide-containing shell as discussed by Anders et al.[26]

Figure 2 shows the particle diameters as a function of annealing temperature as measured by SANS and XRD. It is clear that increasing the annealing temperature leads to a systematic increase in median particle diameter although the diameter determined by SANS increases at a significantly greater rate, particularly at high annealing temperatures. Thus, as the particle arrays are annealed, the results from a combination of these two techniques demonstrate that nanoparticles not only sinter, i.e. coalesce into a single unit

with a common crystallographic axis, but also the sintered particles are able to agglomerate and form larger clusters.

The insert in Fig.1 shows magnetization (at 9 Tesla) of the as-deposited PEI-FePt arrays as a function of measurement temperature. In determining magnetization, the total particle volume was used. The magnetization is significantly reduced from the expected value of ~1000emu/cm^3 and this is now readily explained by the assumption that only the metallic particle core contributes and hence of volume of the magnetically active material is not the same as the total particle volume. These data also show a significant increase in moment at very low temperatures ($T < 20K$). This low temperature increase in moment is also observed for all samples under all annealing conditions, Fig.3a. Modeling our low temperature ($T \leq 20K$) magnetization vs. field data for the as-deposited PEI-FePt arrays using a Langevin function suggests that this increase in measured magnetization is due to an additional population of material that remains superparamagnetic at very low temperatures. This highly superparamagnetic material can be envisioned as particles with a small metallic core of less than 0.8nm diameter or as magnetically de-coupled regions that have only poor crystallographic ordering. This population of highly superparamagnetic material does not contribute to the total moment at $T > 20K$ as the magnetization falls on the linear part of the Langevin curve and is indistinguishable from a paramagnetic background signal. The steep increase in magnetization at low temperature suggests that in the unannealed arrays, this highly superparamagnetic material is much more abundant than the larger 2.2nm magnetic particle cores. The magnetic characteristics of this highly superparamagnetic material were explored further

by fitting a composite function consisting of two Langevin functions to the T = 20K magnetization data. The contribution of the core starts to become hysteretic below T = 20K and so a composite Langevin function cannot be used for the lower temperature data. The parameters obtained from fitting the composite Langevin function to the T = 20K data set a lower bound on the relative particle populations giving a particle number ratio of 10:1 for <0.85nm:2.35nm particles. We speculate that this highly superparamagnetic material is physically located in the Fe-containing oxide shell and are thus available for incorporation into the core without significant chemical reduction.

We now have a physical model of the unannealed particle arrays where data from all the techniques employed can be explained. We use this as a starting point to understand the effects of annealing. Magnetization and H_c measured at room temperature together with coercivity extrapolated to T = 0K (H_0) are shown in Fig. 4 as a function of annealing temperature. There is a strong monotonic increase in both H_c and H_0 with annealing temperature while magnetization initially increases and then decreases. We first consider the magnetization data. The initial increase in magnetization occurs as Fe bound in the oxide shell transforms and becomes incorporated into the magnetic FePt core, shown schematically in Fig.5. The thickness reduction in the oxide-containing shell is shown in the NEXAFS data,[26] by the increase in the metallic Fe peak and reduction in the oxide peaks. Annealing at even higher temperatures allows chemical reactions to occur with the Si substrate to form Fe and/or Pt silicides which reduces magnetization.[26] The formation of Fe silicides has been observed by x-ray diffraction in a series of

nanoparticle arrays annealed at 725°C for 2-120mins. The formation of the silicides is correlated with a significant drop in magnetization.[29]

Figure 3 shows both M_s and H_c for each annealing condition as a function of measurement temperature. The magnetization data above T = 20K decrease only slightly with increasing measurement temperature. Since this is not in a sensitive region of the magnetization vs T curve it is not possible to extract the Curie temperature (T_c) accurately. However, by assuming the bulk values for $L1_0$ or disordered fcc FePt (T_c = 750K and T_c = 710K respectively) gives a value for the total angular momentum (J) of J = 3 which is reasonable when compared with thin films,[30] although in the case of thin films, magnetization drops faster over this temperature range. At low measurement temperatures an increase in magnetization is observed, as noted earlier in the case of the unannealed array. The continued presence of a population of the highly superparamagnetic material suggests that the finite size of the core, ~50 atoms, of these particles inhibits or slows the conversion of Fe in the surrounding shell from Fe-oxide to FePt, or that the composition of the particle is deficient in Pt. We also note that we have no evidence of exchange bias effects in any of the materials studied here.

The coercivity data in Figs. 3 and 4 can be understood in terms of the fraction of the particles which are in the ordered $L1_0$ phase. It was recently shown that for these samples both the fraction of $L1_0$ ordered particles and the degree of ordering within the ordered particles can be extracted from the x-ray diffraction measurements.[26] These data demonstrate that the magnetic particles can, to first order, be divided into two populations, one in the chemically disordered fcc phase which is superparamagnetic and one that is in

a chemically ordered, high anisotropy $L1_0$ phase. In a coercivity measurement, we might then expect to see the two phases, a very low coercivity loop due to the chemically disordered fcc particles, similar to that measured for the unannealed sample (Fig. 1), and a high coercivity loop from the ordered $L1_0$ phase. However, distributions of anisotropy and particle volume together with magnetostatic interactions broaden these transitions. The insert to Fig.4 shows the hysteresis loop for the 580°C/30min annealed sample measured at T = 300K, where a small reduction in M, associated with the superparamagnetic fraction, is observed close to zero applied field. This model of chemically ordered and disordered particles will produce large changes in coercivity, such as those seen in Fig 3 and 4, for only relatively small changes in ordered fraction. In a model system of 3D Stoner Wohlfarth particles we obtain H_0 = 9.2kOe for an order fraction = 0.70 which increases to H_0 = 34kOe for a 0.90 ordered fraction. This corresponds to the order fraction change as the annealing temperature increases from 580°C/30min to 800°C/5mins. We therefore attribute the increase in H_0 to the increase in the fraction of $L1_0$ ordered particles, and not to an increase in the degree of ordering within the particles. This conclusion is supported by x-ray data[26] which demonstrates that particles are either chemically disordered or are essentially ordered. The discrete nature of the ordered and disordered populations is different from the case of FePt thin films,[31] where exchange coupling can effectively average the contribution of regions with different degrees of ordering .

The temperature dependent coercivity data in Fig. 3b can be analyzed in terms of a magnetic activation volume and compared to the particle sizes deduced from XRD and

SANS. This analysis is typically carried out in the framework of the Sharrock equation[32-33] with the assumption of reversal by coherent rotation. Within the Sharrock analysis, H_c is reduced from H_0 due to thermal activation and fitting H_c vs. T determines K_uV where K_u is the anisotropy and V the magnetic, or activation volume. This results in an activation volume which, assuming a spherical particle, gives a diameter of 7.2nm ± 2.0nm. Within error, the magnetic activation volume is qualitatively different from the equivalent XRD and SANS diameters (Fig. 2) and remains nearly constant for all annealing conditions. This suggests that even though the crystallographic particle is growing larger, the volume switched by thermal activation is not, leading to the conclusion that the assumption of reversal by coherent rotation breaks down. Hence as particle diameter increases, reversal proceeds by an incoherent process or by domain nucleation followed by domain wall motion. It should be noted that while the Sharrock approach has proved useful for many magnetic materials, Chantrell et al.,[34] have pointed out that the presence of a superparamagnetic fraction of particles introduces errors into the analysis. We note that since the measured H_0 is reduced due to the superparmagnetic particles, the value of V estimated from the measured H_0 will be too large at low annealing temperatures. Similarly, values of magnetization based on the total physical particle volume, rather than just the magnetically active part, will lead to an over estimation of the activation volume. Determining the uncertainties in magnetization, H_0 and K_uV allows error bars on the calculated activation volume to be estimated. We conclude that given the large increase in physical particle size, the errors introduced into analysis do not affect the conclusions.

IV. CONCLUSIONS

The PEI-FePt polymer mediated process provides good control of nanoparticle array thickness. However, this work demonstrates that a number of critical problems remain before these $L1_0$ nanoparticle arrays can be considered as technological useful data storage materials. The annealing process required to chemically order FePt occurs concurrently with both particle sintering and agglomeration, at least for the PEI-FePt nanoparticle arrays studied here. Control of the unannealed metallic-core / oxide-shell particles forming the array needs to be established, together with control of particle agglomeration through enhanced resistance to particle motion and lower ordering/chemical reduction temperature e.g. through the use of a ternary element. A further requirement, not discussed in this work, is that of magnetic orientation where all particles have a common anisotropy direction. These are significant scientific and technical challenges. However, when resolved, $L1_0$ nanoparticle arrays hold the promise of data storage at one bit/particle corresponding to densities of up to 40Tbit/in^2 and hence pave a way to new paradigms in information technology.

ACKNOWLEDGMENTS

This research was carried out in part at the National Synchrotron Light Source, Brookhaven National Laboratory, which is supported by the U.S. Department of Energy, Division of Materials Sciences and Division of Chemical Sciences, under Contract No. DE-AC02-98CH10886, and in part at the Advanced Light Source, supported by the Office of Basic Energy Sciences, U.S. Department of Energy, under contract # DE-

AC03-76SF00098. We are pleased to acknowledge C.D. Dewhurst of the Institut Laue Langevin in Grenoble, France for help with the SANS measurements and Glenn Held for useful discussions.

References

[1]S. Sun, C.B. Murray, D. Weller, L. Folks and A. Moser, *Science* **287**, 1989 (2000).

[2]H. Zeng, J. Li, J.P. Liu, Z.L. Wang and S. Sun, *Nature* **420**, 395 (2002).

[3]G. V. Kurlyandskaya, M. L. Sanchez, B. Hernando, V. M. Prida, P. Gorria and M. Tejedor, *Appl. Phys. Lett.* **82**, 3053 (2003).

[4]D. K. Kim, M. Mikhaylova, Y. Zhang and M. Muhammed, *Chem. Mater.* **15,** 1617 (2003).

[5]C. Alexiou, A. Schmidt, R. Klein, P. Hulin, C. Bergemann and W. Arnold, *J. Magn. Magn. Mater.* **252**, 363 (2002).

[6]F. Scherer, M. Anton, U. Schillinger, J. Henkel, C. Bergemann, A. Kruger, B. Gansbacher and C. Plank, *Gene Therapy* **9,** 102 (2002).

[7]S. Kang, J. W Harrell and D. E. Nikles, *Nanolett.* **2**, 1033 (2002).

[8]S. Stappert, B. Rellinghaus, M. Acet and E. F. Wassermann, *J. Cryst. Growth* **252**, 440 (2003).

[9]T. Hyeon, *Chem. Comm.* **8**, 927 (2003).

[10]B. Jeyadevan, K. Urakawa, A. Hobo, N. Chinnasamy, K. Shinoda, K. Tohji, D. D. J. Djayaprawira, M. Tsunoda and M. Takahashi, *Jap. J. Appl. Phys. Part 2 Lett.* **42**, L350 (2003).

[11]Y. Huang, H. Okumura, G. C. Hadjipanayis and D. Weller, *J. Magn. Magn. Mater.* **242**, 317 (2002).

[12]T. J. Klemmer, N. Shukla, C. Liu, X. W. Wu, E. B. Svedberg, O. Mryasov, R. W. Chantrell, D. Weller, M. Tanase and D. E. Laughlin, *Appl. Phys. Lett.* **81**, 2220 (2002).

[13]Z. R. Dai, S. Sun, Z. L. Wang, *Surface. Sci.* **505**, 325 (2002).

[14]B. Stahl, J. Ellrich, R. Theissmann, M. Ghafari, S. Bhattacharya, H. Hahn, N. S. Gajbhiye, D. Kramer, R. N. Viswanath, J. Weissmüller and H. Gleiter, *Phys. Rev. B* **67**, 014422 (2003).

[15]S. Sun, D. Weller and C. Murray, in *The Physics of Ultra-High-Density Magnetic Recording* edited by M. L. Plummer, J. v Ek, D. Weller (Springer, New York, 2001).

[16]J. W. Harrell, S. Wang, D. E. Nikles and M. Chen, *Appl. Phys. Lett.* **79**, 4393 (2001).

[17]X. W. Wu, K. Y. Guslienko, R. W. Chantrell and D. Weller, *Appl. Phys. Lett.* **82**, 3475 (2003).

[18]E. Mayes, A. Bewick, D. Gleeson, J. Hoinville, R. Jones, O. Kasyutich, A. Nartowski, B. Warne, J. Wiggins and K. K. W. Wong, *IEEE Trans. Magn.* **39**, 624 (2003).

[19]S. Sun, S. Anders, H. Hamann, J.-U. Thiele, J. E. E. Baglin, T. Thomson, E. E. Fullerton, C. B. Murray and B. D. Terris, *J. Am. Chem. Soc.*, **124**, 2884 (2002).

[20]S. Sun, S. Anders, T. Thomson, J. E. E. Baglin, M. F. Toney, H. Hamann, C. B. Murray and B. D. Terris, *J. Phys. Chem. B.* **107,** 5419 (2003).

[21]P. Lindner, R.P. May and P.A. Timmins, *Physica B* **180 & 181**, 967 (1992).

[22]W.L. Griffith, R. Triolo and A.L. Compere, *Phys. Rev. A* **35**, 2200 (1987).

[23]T. Thomson, S.L. Lee, C.D. Dewhurst, F.Y. Ogrin, C.J. Oates, S.Sun, B.D.Terris, (in preparation).

[24]T. Thomson, S.L. Lee, C.J. Oates, C.D. Dewhurst, F.Y. Ogrin and S. Sun, *ILL Annual Report* 50 (2002).

[25]A. Cebollada, R.F.C. Farrow and M.F. Toney in *Magnetic Nanostructures*, edited by H.S. Nalva (American Scientific Publishers, Stevenson Ranch CA, 2002) pp.93.

[26]S. Anders, M. F. Toney, T. Thomson, J.-U. Thiele, B. D. Terris, S. Sun and C. B. Murray, *J. Appl. Phys.* **93** 6299 (2003).

[27]R. Hayn and V. Drchal, *Phys. Rev. B* **58**, 4341 (1998).

[28]S. Ostanin, S. S. A. Razee, J. B. Staunton, B. Ginatempo and E. Bruno, *J. Appl. Phys.* **93**, 453 (2003).

[29]T. Thomson, M.F.Toney, S.Raoux, J.E.E. Baglin, S.L.Lee, S.Sun and B.D.Terris, *J. Appl. Phys*. (In Press).

[30]S. Okamoto, N. Kikuchi, O. Kitakami, T. Miyazaki, Y. Shimada and K. Fukamichi, *Phys. Rev. B* **66**, 024413 (2002).

[31]M. F. Toney, W-Y. Lee, J. A. Hedstrom and A. Kellock, *J. Appl. Phys.* **93**, 9902 (2003).

[32]M. P. Sharrock and J. T. McKinney, *IEEE Trans. Magn.* **17**, 3020 (1981).

[33]R. H. Victora, *Phys. Rev. Lett.* **63**, 457 (1989).

[34]R. W. Chantrell, D. Weller, T. J. Klemmer, S. Sun and E. E. Fullerton, *J. Appl. Phys.* **91,** 6866 (2002).

Fig.1: M vs H curve at T = 100K for an unannealed nanoparticle array with nominal particle diameters of 4nm. The solid line is a fit to the Langevin function assuming a particle diameter of 2.2nm with Ms = 1030emu/cm^3. Note: the magnetization data at all temperatures above T=20K are well described by a single particle diameter of 2.2nm. The insert shows magnetization at 9 Tesla vs. T normalised to the total particle volume.

Fig.2: Particle diameter for FePt nanoparticles as a function of annealing temperature determined from x-ray diffraction and small angle neutron scattering measurements. The dotted lines are included as a guide to the eye.

Fig.3(a) Magnetization and (b) H_c as a function of measurement temperature for FePt nanoparticle arrays annealed under the different conditions given in the legend. The maximum applied field used was 9 Tesla. The dotted lines are included as a guide to the eye.

Fig.4: Summary of magnetization, H_c and H_0 as a function of annealing temperature. Magnetization and H_c were measured at T=300K and except for the unannealed sample are fully saturated in the maximum applied field of 9 Tesla. The dotted lines are included as a guide to the eye. The insert show the hysteresis loop for the 580°C/30mins annealed sample also measured at T = 300K. The reduction in M close to zero applied field show by the arrow is due to the superparamagnetic fraction of particles.

Fig.5: Schematic illustration of core/shell model of nano-particle array as annealing progresses, showing the increase in the metallic core together with sintering and finally agglomeration. The length scales determined by SANS and XRD are also shown demonstrating the complementary nature of the two techniques.

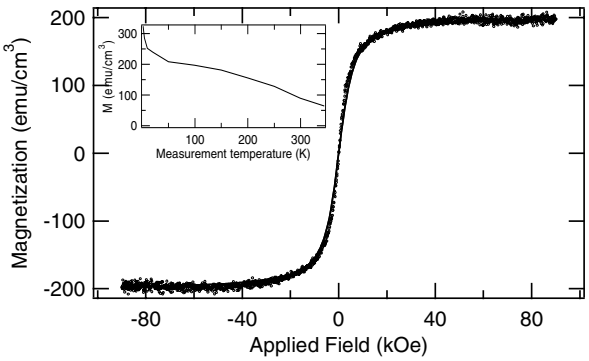
Magnetization (emu/cm^3)
200
100
0
-100
-200
-80
-40
0
40
80
Applied Field (kOe)
M (emu/cm^3)
300
200
100
0
100
200
300
Measurement temperature (K)

Figure 1

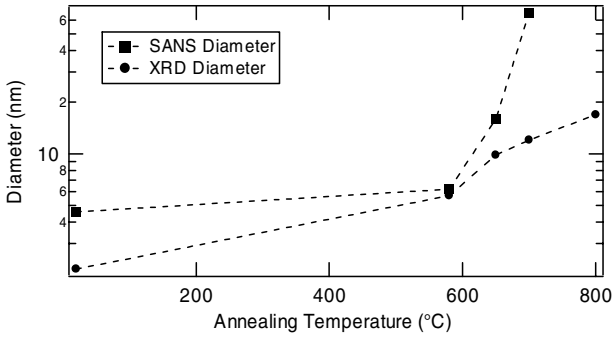
SANS Diameter
XRD Diameter
Diameter (nm)
Annealing Temperature (°C)
200
400
600
800

Figure 2

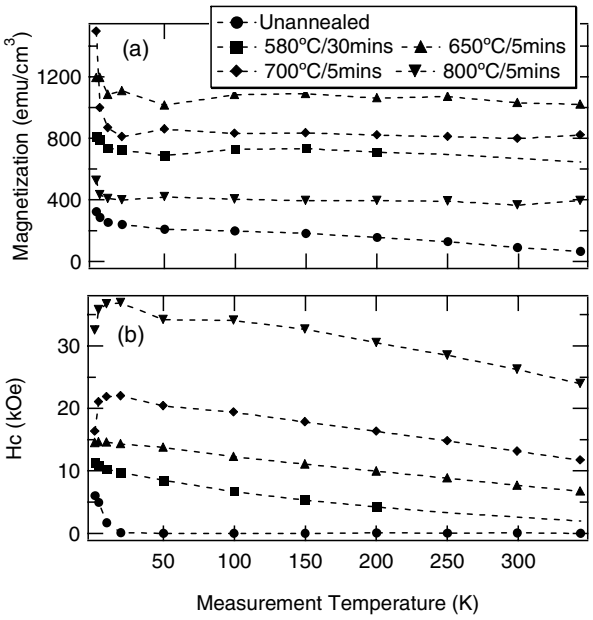
Unannealed
580°C/30mins
650°C/5mins
700°C/5mins
800°C/5mins
(a)
Magnetization (emu/cm3)
1200
800
400
0
(b)
Hc (kOe)
30
20
10
0
50
100
150
200
250
300
Measurement Temperature (K)

Figure 3

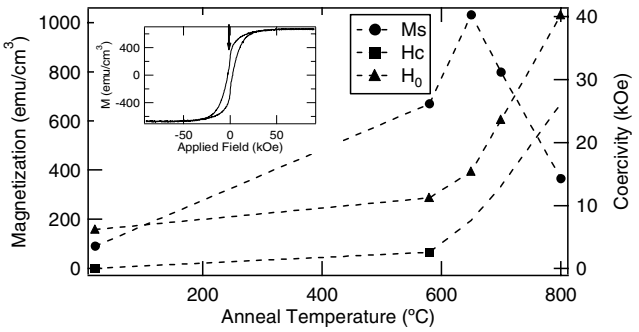
Magnetization (emu/cm^3)
Coercivity (kOe)
Anneal Temperature (°C)
Ms
Hc
H_0
M (emu/cm^3)
Applied Field (kOe)

Figure 4

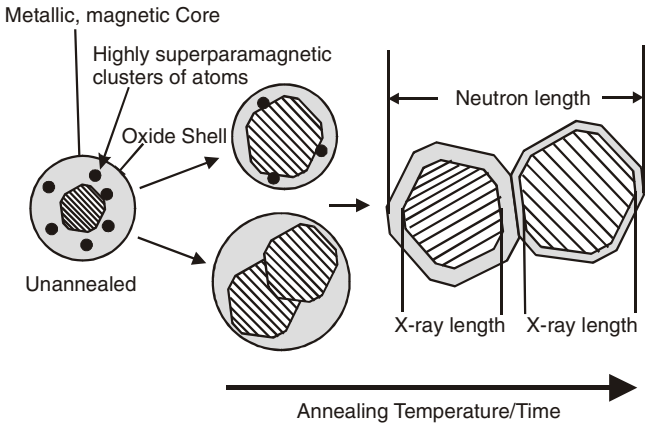
Metallic, magnetic Core
Highly superparamagnetic clusters of atoms
Oxide Shell
Unannealed
Neutron length
X-ray length
X-ray length
Annealing Temperature/Time

Figure 5